

Estimation of Nonlinear ARX Model for Soft Tissue by Wavenet and Sigmoid Estimators

M. A. Ayob¹, W.N.W. Zakaria¹, J. Jalani², N. Mohamed Nasir¹, M. R. Md Tomari¹,

¹*Advanced Mechatronics Research Group (ADMIRE),*

Faculty of Electrical and Electronic Engineering, Universiti Tun Hussein Onn Malaysia.

²*Department of Electrical Engineering Technology,*

Faculty of Engineering Technology, Universiti Tun Hussein Onn Malaysia,

86400 Parit Raja, Batu Pahat, Johor, Malaysia.

mohammadafifayob@gmail.com

Abstract—This paper presents a model-based design technique to estimate the dynamic model of a nonlinear soft tissue phantom using MATLAB Simulink. The soft tissue model was developed using black-box modeling approach; simulations were performed based on acquired set of single input-output data and processed using MATLAB System Identification toolbox. Wavenet and sigmoid estimators were used to acquire the best overall performance. Comparison study has been made between the simulation and experimental results. Our finding shows that the obtained model is sufficient to represent the model of soft tissue phantom with a mean error of 4.12% compared to the real system.

Index Terms—System Identification; Soft Tissue Modeling; RV-2AJ; MATLAB; Simulink; Nonlinear ARX.

I. INTRODUCTION

Model-based design is an approach that allows rapid and cost-effective development of dynamic systems, including control system, signal processing, and communication system. In model-based design, a system model is the main element in the development practice, from essential development through design, execution, and examination [1]. Hence, modeling is acknowledged as the first step of any system analysis and is considered as an important task in scientific studies [2].

Normally, achieving model of a system requires either physical law modeling or via an identification process [3]. However, it is important to realize that physical law modeling often needs hard-to-obtain expert comprehension about the system to be modeled, and thus system identification is introduced. In system identification, a model can be established by preparing a set of measured input and output data without the needs of understanding the system [4], [5]. The identified models can then be used for output prediction, system analysis and diagnostics, system design, and control.

In medical application, stiffness of a human soft tissue has a nonlinear characteristic with uncertainties compared to the stiffness of a hard and linear environment like steel. Therefore, force feedback is often necessary in this research area such as to provide a good and reproducible conduction of an ultrasound signal, while at the same time preventing artery deformation [6]. Furthermore, a haptic interface in minimally invasive surgery is used to produce a trajectory for a surgical

robot and feel contact forces from the working environment [7]. A novel force feedback based tele-operation system for medical application is also presented in [8] and [9]. Other researchers also incorporated force feedback for a medical robot in order to alleviate fatigue in echography [10]. Based on these researches we can conclude that environment stiffness is one of the contributing factors that affect force control performance especially when it involves interaction with human soft tissue.

For that reason, this study discusses on the development of a dynamic simulation model for a generic multipurpose soft tissue phantom through a system identification design technique. MATLAB System Identification toolbox is used to determine the time domain model of the tissue phantom.

II. DESIGNS

Nonlinear ARX (autoregressive exogenous) models describe nonlinear structures using a parallel combination of nonlinear and linear blocks [11]. Previously, various researchers have used nonlinear ARX model for system identification [11]–[15]. The nonlinear and linear functions are expressed in terms of variables called regressors [3]. There are several nonlinear estimators that can be used such as wavelet network, sigmoid network, tree partition, custom network, and neural network. In this study, the performance of wavelet and sigmoid network estimators are chosen and compared due to the simplicity of the structure.

In order to analyze an open system with a classical black-box approach, only the behavior of the stimulus/response is accounted to infer with the unknown box. Hence for better understanding, the representation of a black-box modeling for the soft tissue model is depicted in Figure 1. The input is a depth level of force sensor driven towards the model while the output is the resulted force from the model's deformation. The mathematical model representation is given in Equation (1) and (2).

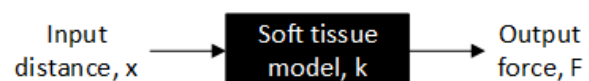


Figure 1: Black-box modeling approach on soft tissue phantom

$$F = kx \quad (1)$$

$$k = \frac{F}{x} \quad (2)$$

The general scheme to determine a dynamic model of a tissue phantom using MATLAB System Identification toolbox involved several stages as illustrated in Figure 2. The initial step is to design the experiment setup for appropriate data collection of system input and output. Afterwards, multiple model structures of nonlinear ARX are generated and chosen based on previous knowledge along with trial and error. Selected models are then identified and validated to see whether they meet the model requirements

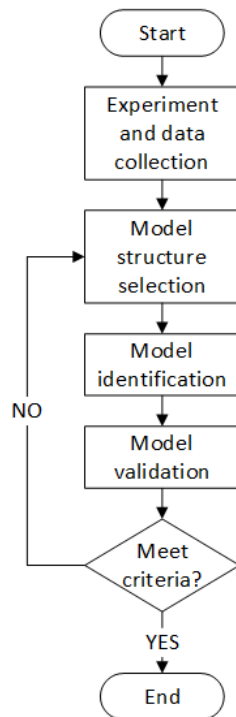


Figure 2: General steps in system identification

A. System Description

Figure 3 shows the interconnection layout of hardware used in the proposed setup. It essentially involved a host computer, an articulated industrial robot arm, and a force/torque (F/T) sensor. In this setup, the output signals from the sensor are collected on the host computer while the input and output of the robot's position is handled using the pendant.

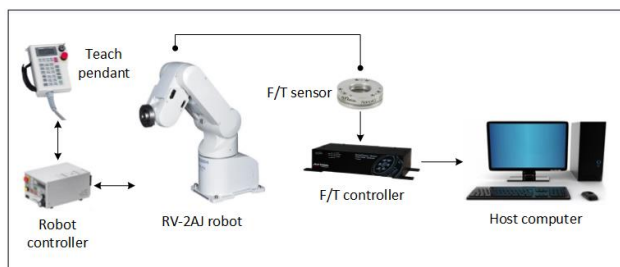


Figure 3: Hardware configuration for data acquisition

The 5-degree of freedom (DOF) RV-2AJ industrial robot arm from Mitsubishi is connected to its controller (Figure 3: Robot controller) with a multi-axis F/T sensor mounted at the robot end effector. The high precision motors with integrated absolute position encoders constantly assured stable operation [16]. In the past, considering that the 17kg compact-sized robot has a repeat position accuracy of $\pm 0.02\text{mm}$, several researchers have used the robot model to develop a master/slave teleoperation system [17], construct a robot simulation software (RSS) using virtual reality interface method [18], control and observe the robot via internet using a client application for a remote access laboratory [19], [20], and inaugurate algorithm for a writing robot [21], [22].

As previously mentioned, the end-effector of the robotic arm is fitted with a near-zero noise distortion six-axis Mini40 F/T sensor from ATI Industrial Automation. The sensor is used to quantify the force acted upon the tissue phantom whenever both of them are in contact. More importantly, the sensor is connected to its controller (Figure 3: F/T controller), where its main purpose is to convert strain gauge data from the sensor to Cartesian components of forces and torques. The sensor which was also attached to a human-like industrial robot was applied to provide force feedback on a human body [6]. The same concept but with a parallel link robot instead was also exercised to alleviate fatigue in echography [10]. Further researches on integrating a F/T sensor to a robotic arm in similar research area has also been worked out for reconstructive surgery [23]–[25], developing a skincare robot [26], assisting lung motion compensation during needle insertion [27], estimating needle deflection during soft-tissue needle insertion [28], and developing rehabilitation robot for wrist rotation [29].

B. Data Acquisition

The first step in system identification modeling is to identify and gather relevant data from both robot and tissue phantom. Therefore the data collection setup is presented in Figure 4. We have determined the input of the model to be the distance of the robot's end effector travel towards the tissue phantom and the output is reaction force component of the phantom. To acquire the corresponding data, the robot was programmed manually via the teach pendant to move starting from the surface of the phantom with increments of 0.5mm until it reaches 10mm of travel while the force component at each increments are recorded simultaneously. The process is repeated until desired amount of data are achieved.



Figure 4: Data acquisition setup for tissue phantom

In this research, only z-axis force data are gathered since our main concern is to develop force control on this axis and position control on x and y-axis [30]–[32]. Additionally, communication between the F/T controller to the host computer was set using serial RS-232 connection at a baud rate of 9600Bd with sampling rate of 2500Hz. The resulted input and output data for the experimental setup is shown accordingly as in Figure 5.

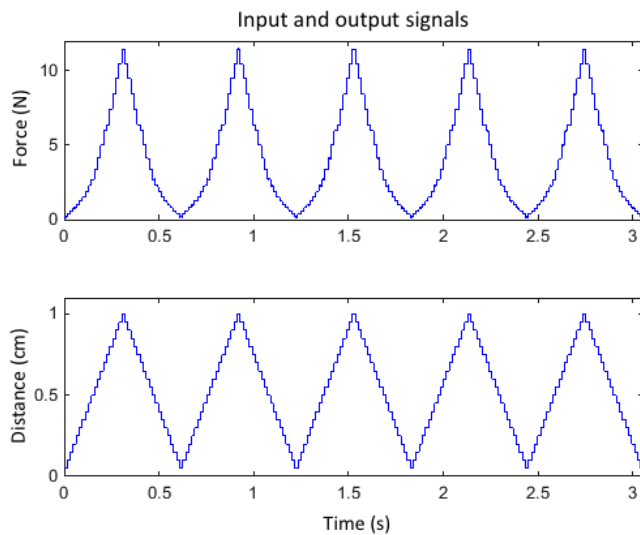


Figure 5: Input signals (robot travel towards phantom) and output signals (acting force towards robot)

III. SIMULATION RESULTS AND ANALYSIS

A. Model Identification

In the System Identification toolbox, half portion from a total of 3820 acquired data was selected for data evaluation while the other half for data validation. Nonlinear ARX model estimation with wavenet and sigmoid network estimator was chosen to study which of both estimators will result in better model identification. Table 1 shows the comparison outcome between different model structures with summary on the best fit percentage, autocorrelation function (ACF) and cross correlation function (CCF). Multiple sets of model structures were used to estimate the system model up to 3 terms of output [na], input [nb] and delay [nk].

B. Model Validation

In order to validate the authenticity of the model, the best fitting between the simulation response of the identified model and the actual plant was recognized. Essentially, model with best fit percentage signifies how much that model is able to represent the actual system.

Apart from the best fit, autocorrelation of residuals and cross correlation analysis were examined as well. The confidence level for both correlations was set at 95% (p-value of 0.05). Models with good performance should have the response within this limit but if the response deviates 5-10% out of range, it is still considered as good while over 10% is accounted as poor.

Based on test results in Table 1, we have concluded that sigmoid estimator produces the best nonlinear ARX model at [2 2 0] model structure. The model fit is relatively high at 96.23% and it passes both the ACF and CCF analysis. Comparison between actual and simulated model output is presented in Figure 6 while Figure 7 shows the autocorrelation and cross correlation analysis.

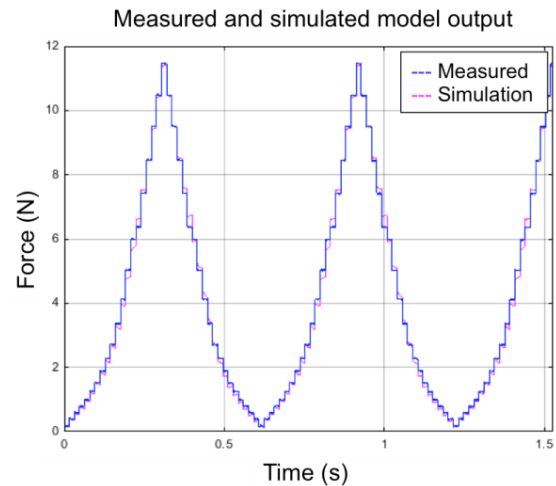


Figure 6: Simulation and actual response of system output

Table 1

Model fit and correlation test summary for nonlinear models using wavenet and sigmoid estimators

Model Structure [na nb nk]	Wavenet Estimator			Sigmoid Estimator		
	Model Fit, %	A CF	C CF	Model Fit, %	A CF	C CF
0 1 0	99.40	X	X	99.40	X	X
0 1 1	95.42	O	X	95.43	O	X
0 1 2	93.55	X	X	93.56	X	X
1 1 0	99.40	X	X	99.40	X	X
1 1 1	-137.90	O	X	41.51	O	X
1 1 2	93.55	X	X	-19.73	O	X
2 1 0	15.18	X	X	97.17	X	X
2 1 1	-109.20	O	X	0	O	X
2 1 2	-111.90	O	X	0	O	X
3 1 0	90.97	X	X	96.04	X	X
3 1 1	-93.20	O	X	0	O	X
3 1 2	-342.50	O	X	0	O	X
0 2 0	97.62	X	X	97.28	X	X
0 2 1	95.15	X	X	94.73	X	X
0 2 2	93.31	X	X	93.05	X	X
1 2 0	-2446	X	X	78.23	X	X
1 2 1	-130.50	O	X	64.60	O	X
1 2 2	-122.80	O	X	0	O	X
2 2 0	68.82	O	O	96.23	O	O
2 2 1	-576.80	O	X	62.76	O	X
2 2 2	-122.20	O	X	56.89	O	X
3 2 0	68.63	O	O	91.74	X	X
3 2 1	-634.40	O	X	64.32	O	X
3 2 2	-505.90	O	X	73.64	O	X
0 3 0	93.66	X	X	96.69	X	O
0 3 1	84.95	X	X	94.44	X	X
0 3 2	93.32	X	X	92.89	X	X
1 3 0	70.94	O	O	92.69	X	X
1 3 1	-139.10	O	X	79.12	O	X
1 3 2	-25.50	O	X	29.28	O	X
2 3 0	70.34	O	O	95.10	X	X
2 3 1	-482.80	O	X	61.27	O	X
2 3 2	-158.7	O	X	70.36	O	X
3 3 0	69.95	O	O	35.87	X	X
3 3 1	-756	O	X	-810.40	O	X
3 3 2	-324.60	O	X	-28.35	O	X

Legend: O means pass while X means fail. Shaded values indicate model structure with pass in both ACF and CCF.

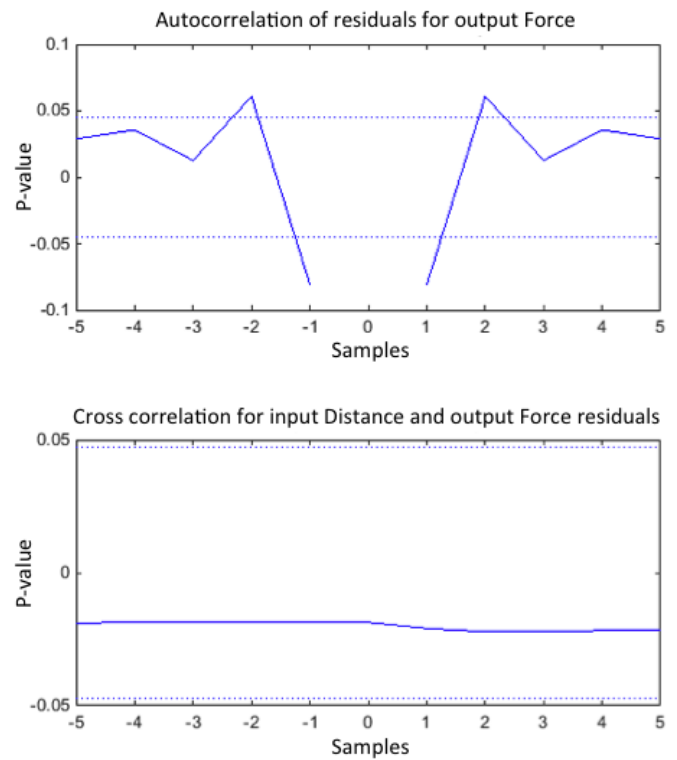


Figure 7: Autocorrelation and cross correlation analysis for [2 2 0] nonlinear ARX sigmoid estimator

Comparison of final mean value between the measured and simulation data is given in Figure 8 while the exact values and difference errors are listed in Table 2. From the given graph we can see that the nonlinearity curve of the simulated model closely resembles the measured point from the experiment. The mean error of the simulated model on the other hand only produces 4.12% indicating the high accuracy of the selected nonlinear ARX model structure.

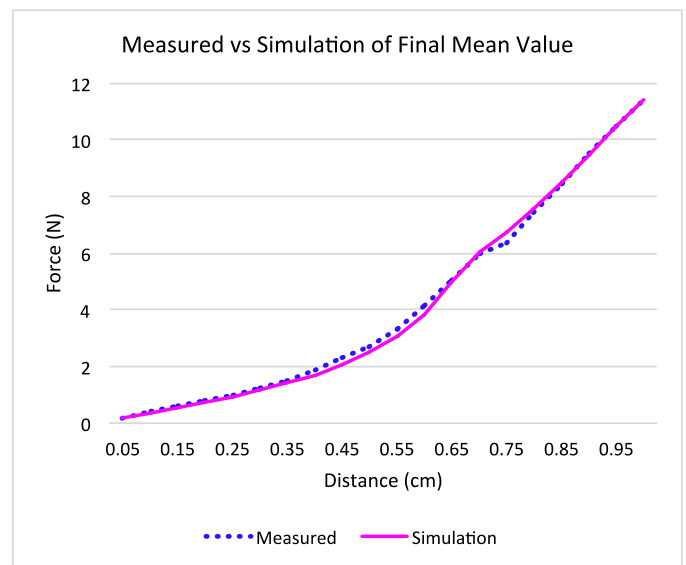


Figure 8: Measured vs simulation of final mean value

Table 2
Measured and simulation output force at fixed input distance

Input Distance (cm)	Output Force (N)		Error (%)
	Measured	Simulation	
0.05	0.1675	0.1777	6.06
0.10	0.3935	0.3549	9.82
0.15	0.5895	0.5259	10.79
0.20	0.7849	0.7034	10.39
0.25	0.9877	0.9152	7.34
0.30	1.2431	1.1600	6.69
0.35	1.5194	1.4120	7.07
0.40	1.8907	1.6940	10.40
0.45	2.2825	2.0420	10.54
0.50	2.7048	2.4780	8.38
0.55	3.3528	3.0440	9.21
0.60	4.1174	3.8510	6.47
0.65	5.0153	4.9970	0.37
0.70	5.9738	6.0330	0.99
0.75	6.3653	6.7690	6.34
0.80	7.4116	7.5350	1.66
0.85	8.4368	8.4920	0.65
0.90	9.4982	9.4660	0.34
0.95	10.4597	10.4400	0.19
1.00	11.4357	11.4200	0.14
Mean Error			4.12

$$\text{Legend: Error} = \frac{|\text{Measured} - \text{Simulation}|}{\text{Measured}} \times 100\%$$

IV. CONCLUSION

In this study, the model-based design approach of a generic multipurpose tissue phantom has been presented. The proposed setup uses MATLAB System Identification toolbox to develop the simulation model of a tissue phantom. Based on the earlier findings, the highest best fit of a simulated model produced from the toolbox does not necessarily means the best overall model. Autocorrelation and cross correlation function has to be considered as well.

Simulation study has been conducted to validate the selected nonlinear ARX model structure based on a high best fit and a pass in correlation analysis. From the results and comparisons, [2 2 0] model structure using sigmoid estimator happened to be the best model that closely resembles the real system with relatively low mean error of 4.12%.

Lastly, this work has demonstrated that model-based design practice that incorporates tasks of system identification is a straightforward process when done correctly in MATLAB Simulink environment. In our research, force control can be developed in later stages considering that we have obtained the model and characteristics of the soft tissue phantom. By using a model of real tissue phantom for simulation purposes, we could develop a robot-assisted surgical system that would comply with any human tissues and body parts once the tissue characteristics are recognized.

ACKNOWLEDGMENT

This work was supported by Ministry of Education and Universiti Tun Hussein Onn Malaysia under Research Acculturation Grant Scheme Vot R032.

REFERENCES

- [1] MATLAB, "Model-Based Design." [Online]. Available: <http://www.mathworks.com/help/simulink/gs/model-based-design.html>. [Accessed: 03-Oct-2015].
- [2] H. Shakouri G. and H. R. Radmanesh, "Identification of a continuous time nonlinear state space model for the external power system dynamic equivalent by neural networks," *Int. J. Electr. Power Energy Syst.*, vol. 31, no. 7-8, pp. 334-344, 2009.
- [3] L. Ljung, Ed., *System Identification (2Nd Ed.): Theory for the User*. Upper Saddle River, NJ, USA: Prentice Hall PTR, 1999.
- [4] H. J. Palanthandalam-Madapusi, S. Lacy, J. B. Hoagg, and D. S. Bernstein, "Subspace-Based Identification for Linear and Nonlinear Systems," *Am. Control Conf.*, p. 15, 2005.
- [5] T. G. Ling, M. F. Rahmat, a. R. Husain, and R. Ghazali, "System identification of electro-hydraulic actuator servo system," in *2011 4th International Conference on Mechatronics (ICOM)*, 2011, no. May, pp. 1-7.
- [6] F. Pierrot, E. Dombre, E. Dégoullange, L. Urbain, P. Caron, S. Boudet, J. Gariépy, and J.-L. Mègnien, "Hippocrate: a safe robot arm for medical applications with force feedback," *Med. Image Anal.*, vol. 3, no. 3, pp. 285-300, Sep. 1999.
- [7] C. Preusche, T. Ortmaier, and G. Hirzinger, "Teleoperation concepts in minimal invasive surgery," *Control Eng. Pract.*, vol. 10, no. 11, pp. 1245-1250, Nov. 2002.
- [8] G. Song and S. Guo, "A novel force feedback-based teleoperation system for medical application," *Int. J. Innov. Comput. Inf. Control*, vol. 3, no. 3, pp. 737-750, 2007.
- [9] J. Park, "A Haptic Teleoperation Approach Based on Contact Force Control," *Int. J. Rob. Res.*, vol. 25, no. 5-6, pp. 575-591, May 2006.
- [10] K. Masuda, Y. Urayama, S. Saito, and Y. Takachi, "Development of cooperate system with medical robot to alleviate fatigue in echography," in *The 4th 2011 Biomedical Engineering International Conference*, 2012, pp. 161-164.
- [11] N. Ismail, N. Tajjudin, M. H. F. Rahiman, and M. N. Taib, "Estimation of nonlinear ARX model for steam distillation process by wavenet estimator," in *2009 IEEE Student Conference on Research and Development (SCORED)*, 2009, pp. 562-565.
- [12] Y. Hasuikie, M. Izutsu, and S. Hatakeyama, "A Identification Method of a nonlinear ARX Model with Variable Order for Nonlinear Systems," pp. 3244-3249.
- [13] C. Galván-Duque, R. Zavala-Yoé, G. Rodríguez-Reyes, F. Mendoza-Cruz, and R. Ramírez, "Classical and intelligent ARX models for classification of gait events," *Proc. - 2013 Int. Conf. Mechatronics, Electron. Automot. Eng. ICMEAE 2013*, pp. 78-83, 2013.
- [14] Z. Li, M. Hayashibe, Q. Zhang, and D. Guiraud, "FES-induced muscular torque prediction with evoked EMG synthesized by NARX-type recurrent neural network," *IEEE Int. Conf. Intell. Robot. Syst.*, pp. 2198-2203, 2012.
- [15] N. Shamsuddin and M. N. Taib, "Nonlinear ARX modeling of heart diseases based on heart sounds," *Signal Process. its Appl. (CSPA)*, 2011 *IEEE 7th Int. Colloq.*, pp. 382-387, 2011.
- [16] M. F. M. Esa, H. Ibrahim, N. H. Mustaffa, and H. A. Majid, "The Mitsubishi MelfaRxm middleware and application: A case study of RV-2AJ robot," in *2011 IEEE Conference on Sustainable Utilization and Development in Engineering and Technology (STUDENT)*, 2011, no. October, pp. 138-143.
- [17] M. Mamdouh and A. a. Ramadan, "Development of a teleoperation system with a new workspace spanning technique," *2012 IEEE Int. Conf. Robot. Biomimetics*, pp. 1570-1575, Dec. 2012.
- [18] M. I. Jambak, H. Haron, and D. Nasien, "Development of Robot Simulation Software for Five Joints Mitsubishi RV-2AJ Robot Using MATLAB/Simulink and V-Realm Builder," *2008 Fifth Int. Conf. Comput. Graph. Imaging Vis.*, pp. 83-87, Aug. 2008.
- [19] J. a. Buitrago, F. D. Giraldo, and J. a. Lamprea, "Remote access lab for Mitsubishi RV-2AJ robot," *IX Lat. Am. Robot. Symp. IEEE Colomb. Conf. Autom. Control. 2011 IEEE*, pp. 1-7, Oct. 2011.
- [20] M. F. Crainic and S. Preitl, "Virtual laboratory for a remotely operating robot arm," *SACI 2014 - 9th IEEE Int. Symp. Appl. Comput. Intell. Informatics, Proc.*, no. 1, pp. 101-104, 2014.
- [21] S. Yussof, A. Anuar, and K. Fernandez, "Algorithm for robot writing using character segmentation," in *Proceedings - 3rd International Conference on Information Technology and Applications, ICITA 2005*, 2005.

- [22] M.-F. Crainic, S. Preitl, L. A. Sandru, and V. Dolga, "Secure handwriting using a robot arm for educational purpose," *Methods and Models in Automation and Robotics (MMAR), 2014 19th International Conference On*, pp. 58–63, 2014.
- [23] E. Dombre, G. Duchemin, P. Poignet, and F. Pierrot, "Dermarob: a safe robot for reconstructive surgery," *IEEE Trans. Robot. Autom.*, vol. 19, no. 5, pp. 876–884, 2003.
- [24] F. Pierrot, E. Dombre, L. Teot, and E. Degoulange, "Robotized reconstructive surgery: ongoing study and first results," *Proc. IEEE Int. Conf. Robot. Autom.*, no. April, pp. 1615–1620, 2000.
- [25] G. Duchemin, P. Maillet, P. Poignet, E. Dombre, and F. Pierrot, "A hybrid position/force control approach for identification of deformation models of skin and underlying tissues," *IEEE Trans. Biomed. Eng.*, vol. 52, no. 2, pp. 160–170, 2005.
- [26] Y. Tsumaki, T. Kon, A. Suginuma, K. Imada, A. Sekiguchi, D. N. Nenchev, H. Nakano, and K. Hanada, "Development of a skincare robot," *2008 IEEE Int. Conf. Robot. Autom.*, pp. 2963–2968, 2008.
- [27] S. F. Atashzar, I. Khalaji, M. Shahbazi, A. Talasaz, R. V. Patel, and M. D. Naish, "Robot-assisted lung motion compensation during needle insertion," *2013 IEEE Int. Conf. Robot. Autom.*, pp. 1682–1687, 2013.
- [28] T. Lehmann, C. Rossa, N. Usmani, R. Sloboda, and M. Tavakoli, "A virtual sensor for needle deflection estimation during soft-tissue needle insertion," in *2015 IEEE International Conference on Robotics and Automation (ICRA)*, 2015, pp. 1217–1222.
- [29] H. M. Kim, T. K. Hong, and G. S. Kim, "Design of a wrist rotation rehabilitation robot," *4th Annu. IEEE Int. Conf. Cyber Technol. Autom. Control Intell.*, pp. 240–245, 2014.
- [30] M. A. Ayob, W. N. W. Zakaria, and J. Jalani, "Forward kinematics analysis of a 5-axis RV-2AJ robot manipulator," in *Electrical Power, Electronics, Communications, Controls and Informatics Seminar (EECCIS), 2014*, 2014, pp. 87–92.
- [31] M. A. Ayob, W. N. Wan Zakaria, J. Jalani, and M. R. Md Tomari, "Inverse kinematics analysis of a 5-axis RV-2AJ robot manipulator," *ARNP J. Eng. Appl. Sci.*, vol. 10, no. 18, pp. 8388–8394, 2015.
- [32] M. A. Ayob, W. N. Wan Zakaria, J. Jalani, and M. R. Md Tomari, "MODELING AND SIMULATION OF A 5-AXIS RV-2AJ ROBOT USING SIMMECHANICS," *J. Teknol.*, vol. 76, no. 4, pp. 59–63, Sep. 2015.